Constraining kernel estimators in semiparametric copula mixture models

Gildas Mazo, Yaroslav Averyanov

Constraining kernel estimators in semiparametric copula mixture models

Gildas Mazo[1] Yaroslav Averyanov[2]

[1]MaIAGE, INRA, Université Paris-Saclay, 78350, Jouy-en-Josas, France
[2]MODAL, Inria Lille Nord Europe, Lille, France

Abstract

This paper presents a novel algorithm for performing inference and/or clustering in semiparametric copula-based mixture models. The algorithm replaces the standard kernel density estimator by a weighted version that permits to take into account the constraints put on the underlying marginal densities. Lower misclassification error rates and better estimates are obtained on simulations. The pointwise consistency of the weighted kernel density estimator is established under an assumption on the rate of convergence of the sample maximum.

Keywords: copula; kernel; semiparametric; nonparametric; mixture model; clustering.

1 Introduction

In modern data science, the observations of heterogeneous clusters is not uncommon. An example is given in [4] where one can observe two heterogeneous clusters of data points described by blood pressure and medical costs. The first dimension has a skewed Gaussian distribution and the second a log-normal distribution. The first cluster has negative dependency and the second positive dependency. These data cannot be captured by the standard Gaussian mixture model. The Student-t mixture model [10][15] is not able to deal with heterogeneous clusters either.

Recently more flexible models have been considered. On the one hand, there are copula-based methods. Copula-based methods allow for a separate analysis of the marginals and the dependence structure. They have been successfully applied in Pattern Recognition [23], Machine Learning [22], Knowledge Discovery and Database Management [4]. Copulas allow for concatenating discrete and continuous data, too [13]. For a statistical perspective, see e.g. [9, 8].

On the other hand, there are nonparametric methods. Nonparametric methods do not need to pick parametric families for the component distributions (i.e., the distributions of the clusters) but at the cost of assuming independence within each component [1, 12]. In nonparametric mixture models, the parameters are probability density functions, which are estimated by kernel density estimators embedded in pseudo-EM algorithms [2].

In this paper, following the work in [14], we combine both the copula framework and nonparametric estimation into a single mixture model. This permits to capture a wide spectrum of dependence structures while avoiding the choice of setting up the parametric families for the marginals. However, there is an important difference between the model of [14] and ours. In the former, the distributions in the clusters were not allowed to vary in scale. In the latter, change in scale is possible. This additional degree of freedom induces a structural constraint on the component marginal densities of the mixture. The constraint is not satisfied by the kernel density estimator used in the algorithm in [14]. How can we take the constraint into account? Will the inference be improved? To answer the first question, we have built a random weighted kernel density estimator and proved its pointwise consistency. To answer the second, we compared the algorithms on simulated and real data.

The rest of this paper is as follows. We present the models in Section 2. The first part reviews the paradigms under which one can build mixture models (Gaussian, copula-based, nonparametric and semiparametric) and the second part presents the model of interest in this paper. We give the learning algorithms in Section 3. Section 4 contains the definition and the consistency result for the weighted kernel density estimator. This section is written in a generic framework and therefore can be read independently. Section 5 and Section 6 contain the simulation experiments and the real data analysis, respectively. A Summary closes the paper.

2 Four kinds of mixture models

2.1 A review of paradigms for mixture models

We consider mixture models of the form

$$f(x_1, \ldots, x_d) = \sum_{z=1}^{K} \pi_z f_z(x_1, \ldots, x_d), \tag{1}$$

where $\pi_1, \ldots, \pi_K$ are the proportions of the K components (or clusters) and $f_1, \ldots, f_K$ are the corresponding densities. The choice of the structure for the component densities f_z specifies the kind of mixture model.

The first kind of mixture model is as follows. One picks a multivariate parametric family for the component densities and estimate their parameters by maximum likelihood through an EM algorithm. In the majority of cases one usually picks the multivariate Gaussian family, or, perhaps, the multivariate Student-t family. Note that all coordinates of a vector of variables are distributed according to the same distribution up to their parameters. For instance, all the coordinates of a vector distributed according to a Gaussian mixture model are Gaussian. This is an homogeneity assumption. We refer to a standard textbook [15] for further details.

The second kind of mixture model arises when one chooses to use the copula decomposition for each of the component densities, that is, one writes

$$f_z(x_1, \ldots, x_d) = c_z(F_{1,z}(x_1), \ldots, F_{d,z}(x_d)) \prod_{j=1}^{d} f_{j,z}(x_j), \tag{2}$$

where c_z is the copula density corresponding to, and $f_{1,z}, \ldots, f_{d,z}$ are the marginals of, f_z. Here $F_{1,z}, \ldots, F_{d,z}$ are the corresponding (cumulative) distribution functions. Sklar's theorem [25, 16] states that for any distribution function F_z with continuous marginals $F_{1,z}, \ldots, F_{d,z}$, there exists a function $C_z : [0,1]^d \to [0,1]$, called the copula, such that

$$F_z(x_1, \ldots, x_d) = C_z(F_{1,z}(x_1), \ldots, F_{d,z}(x_d)), \tag{3}$$

for any $(x_1, \ldots, x_d)$ in the domain of definition of F_z. The decomposition (2) follows from Sklar's theorem by differentiation. The copula C_z encodes the dependence structure of a random vector. One easily checks that C_z is the distribution function of the random vector $(F_{1,z}(X_1), \ldots, F_{d,z}(X_d))$ if F_z is the distribution function of $(X_1, \ldots, X_d)$. Copulas are typically parametrized by considering families of the form $\{C_z(\cdot, \ldots, \cdot; \theta_z), \theta_z\}$ for some parameters θ_z. An example is given in Section 5. If in (3) $C_z(u_1, \ldots, u_d) = u_1 \cdots u_d$, then $c_z = 1$ in (2). This means that the variables are independent conditionally on belonging to the cluster z. In copula-based models, one can choose different parametric families for the marginals within the same cluster but this heterogeneity property comes at a price. Indeed, the specification of all the parametric families (there are dK marginals) can be a daunting task. Estimation of copula-based mixture models can be performed by EM or EM-like algorithms [9].

The third kind of mixture model is of nonparametric flavor. In nonparametric mixture models, one assumes

$$f(x_1, \ldots, x_d) = \sum_{z=1}^{K} \pi_z \prod_{j=1}^{d} f_{j,z}(x_j).$$

That is, conditionally on the labels (i.e. conditionally on being in a certain cluster), the variables are assumed to be independent. But, in contrast to copula-based mixture models, one does not assume parametric marginals. Nonparametric estimation can be performed with kernel density estimators embedded in EM-like algorithms [1]. In [1], marginals of the form

$$f_{j,z}(x_j) = \frac{1}{\sigma_{j,z}} g_j\left(\frac{x_j - \mu_{j,z}}{\sigma_{j,z}}\right), \tag{4}$$

where $\mu_{j,z}$ and $\sigma_{j,z}$ are location and scale parameters, respectively, are also considered. The case $\sigma_{j,z} = 1$ and $d = 1$ was considered in [2]. This work largely inspired further work on nonparametric mixture models from the kernel density estimation viewpoint. But nonparametric maximum likelihood estimation is also possible if one assumes log-concavity of the component densities [7].

The fourth kind of mixture model combines nonparametric estimation and copula modeling [14]. It is of the form (1), (2) and (4). In (2), the distribution functions $F_{j,z}$ are given by $F_{j,z}(x_j) = G_j((x_j - \mu_{j,z})/\sigma_{j,z})$ and

$$G_j(x_j) = \int_{-\infty}^{x_j} g_j(t)\,\mathrm{d}t. \tag{5}$$

The model [14] is a particular case where $\sigma_{j,z} = 1$. The g_j (hereafter called the *generators*) are estimated in a nonparametric way but the copula are entirely parametric, thus the term semiparametric used for this kind of models. Inference

can be performed with essentially the same algorithms as in [1, 2] but with an additional step for estimating the copula parameters. Algorithm 1 in Section 3 is an example of such algorithms.

2.2 The model of interest

We consider a model of the fourth kind, a so called location-scale semiparametric copula-based mixture model of the form

$$f(x_1,\dots,x_d)=\sum_{z=1}^{K}\pi_z c_z\left(G_1\left(\frac{x_1-\mu_{1,z}}{\sigma_{1,z}}\right),\dots,G_d\left(\frac{x_d-\mu_{d,z}}{\sigma_{d,z}}\right)\right)\prod_{j=1}^{d}\frac{1}{\sigma_{j,z}}g_j\left(\frac{x_j-\mu_{j,z}}{\sigma_{j,z}}\right),$$

that is, of the form (1), (2) and (4) where the generators g_j, $j=1,\dots,d$, satisfy

$$\int x_j g_j(x_j)\,\mathrm{d}x_j=0 \tag{6}$$

and

$$\int x_j^2 g_j(x_j)\,\mathrm{d}x_j=1. \tag{7}$$

Note that there is no loss of generality in assuming a unit variance in (7). Indeed, if the variance would be σ_j^2, say, then we could find a unique reparametrization (given by $\tilde{g}_j(x_j)=\sigma_j g_j(\sigma_j x_j)$ and $\tilde{\sigma}_{j,z}=\sigma_j\sigma_{j,z}$) so that (7) would be true. The copulas are parametrized by vectors θ_z. No specific parametric families are assumed for the generators.

3 Estimation

Given the model of interest in Section 2.2, one needs to estimate the proportions π_z, locations $\mu_{j,z}$, scales $\sigma_{j,z}$, generators g_j and copulas parameters θ_z for $z=1,\dots,K$ and $j=1,\dots,d$. Note that the estimates of the distribution functions G_j can be computed through (5). The sample is denoted by $(x_1^{(i)},\dots,x_d^{(i)})$, $i=1,\dots,n$. Two learning algorithms are presented in this section. Algorithm 1, is essentially the same as that in [14], which itself is inspired from the algorithms in [1, 2]. Hence we do not consider that Algorithm 1 is a contribution of the paper. The contribution is Algorithm 2.

Building upon the work of [2, 1, 14], the most natural algorithm one can build is Algorithm 1. Algorithm 1 requires initial estimates $\pi_z^0,\mu_{j,z}^0,\sigma_{j,z}^0,g_j^0,\theta_z^0$ and then produces a sequence $\pi_z^t,\mu_{j,z}^t,\sigma_{j,z}^t,g_j^t,\theta_z^t$, for $t=1,2,\dots$ until some stopping criterion has been reached. The first step is similar to the E step of any EM algorithm. The second step is also similar to the EM algorithm for Gaussian mixture models: the parameters are updated by computing weighted means where the weights $w_{i,z}^t$ relate the observations to their probabilities of belonging to the given clusters. The third step is similar to the computations undertaken in [2]. Given the data $x_j^{(i)}$ and given the weights computed at the t-th iteration, one generates a random label $Z^i\in\{1,\dots,K\}$ according to a multinomial distribution Multi$(w_{i,1}^t,\dots,w_{i,d}^t)$. One then standardizes the data according to these simulated labels, that is, builds a pseudo-sample $\tilde{x}_j^{(1)},\dots,\tilde{x}_j^{(n)}$ and constructs a

Algorithm 1

Given initial estimates $\pi_z^0, \mu_{j,z}^0, \sigma_{j,z}^0, g_j^0, \theta_z^0$ and for $t = 1, 2, \ldots$ (until some stopping criterion has been reached), follow the steps below.

1. Compute (for $i = 1, \ldots, n$ and $z = 1, \ldots, K$)

$$w_{i,z}^t = \frac{\pi_z^t c_z \left\{ G_1^t \left(\frac{x_1^{(i)} - \mu_{1,z}^t}{\sigma_{1,z}^t} \right), \ldots, G_d^t \left(\frac{x_d^{(i)} - \mu_{d,z}^t}{\sigma_{d,z}^t} \right); \theta_z^t \right\} \prod_{j=1}^d \frac{1}{\sigma_{j,z}^t} g_j^t \left(\frac{x_j^{(i)} - \mu_{j,z}^t}{\sigma_{j,z}^t} \right)}{\sum_{z=1}^K \pi_z^t c_z \left\{ G_1^t \left(\frac{x_1^{(i)} - \mu_{1,z}^t}{\sigma_{1,z}^t} \right), \ldots, G_d^t \left(\frac{x_d^{(i)} - \mu_{d,z}^t}{\sigma_{d,z}^t} \right); \theta_z^t \right\} \prod_{j=1}^d \frac{1}{\sigma_{j,z}^t} g_j^t \left(\frac{x_j^{(i)} - \mu_{j,z}^t}{\sigma_{j,z}^t} \right)}$$

2. Process through the following steps ($j = 1, \ldots, d$, $z = 1, \ldots, K$).

   (a) Update the cluster proportions

$$\pi_z^{t+1} = \frac{1}{n} \sum_{i=1}^n w_{i,z}^t.$$

   (b) Update the location parameters

$$\mu_{j,z}^{t+1} = \frac{\sum_{i=1}^n x_j^{(i)} w_{i,z}^t}{\sum_{i=1}^n w_{i,z}^t}.$$

   (c) Update the scale parameters

$$(\sigma_{j,z}^{t+1})^2 = \frac{\sum_{i=1}^n (x_j^{(i)} - \mu_{j,z}^t)^2 w_{i,z}^t}{\sum_{i=1}^n w_{i,z}^t}.$$

3. To update the generators, proceed through the following steps ($j = 1, \ldots, d$).

   (a) Generate a random variable $Z^{(i)}$ from Multi$(w_{i,1}^t, \ldots, w_{i,K}^t)$,

   (b) Define $\tilde{x}_j^i = (x_j^i - \mu_{j,Z^{(i)}}^t)/\sigma_{j,Z^{(i)}}^t$.

   (c) Choose a bandwidth h_j and update the generators

$$g_j^{t+1}(x_j) = \frac{1}{nh_j} \sum_{i=1}^n K \left(\frac{x_j - \tilde{x}_j^{(i)}}{h_j} \right) \tag{8}$$

4. Update the copula parameters ($z = 1, \ldots, K$)

$$\boldsymbol{\theta}_z^{t+1} = \arg\max_{\boldsymbol{\theta}_z} \sum_i w_{i,z}^t \log c_z \left\{ G_1^{t+1} \left(\frac{x_1^{(i)} - \mu_{1z}^{t+1}}{\sigma_{1,z}^{t+1}} \right), \ldots, G_d^{t+1} \left(\frac{x_d^{(i)} - \mu_{dz}^{t+1}{}^{t+1}}{\sigma_{d,z}} \right); \boldsymbol{\theta}_z \right\}$$

kernel density estimator on the top of it for updating the generators. The kernel density estimator can be constructed by following the guidelines as those in a standard textbook [24]. In (8), the kernel is denoted by K and the bandwidth by h_j. Thanks to a straightforward extension of Lemma 1 in [2], one has that, at each iteration t of the algorithm, $\tilde{x}_j^{(1)}, \ldots, \tilde{x}_j^{(n)}$ is a sample from g_j^t and therefore the choice of the bandwidth can be based on that sample. Finally in the last step, one maximizes a pseudo-likelihood for the copula parameters. See [14] for more details about this step. Algorithm 1 empirically has been found to perform well on simulations (see Section 5) whenever one is concerned with the estimation of the parameters for their own sake. However, when one is interested in the task of clustering instead, Algorithm 1 appears to have no greater value than a standard Gaussian mixture model. See Figure 1 and Section 5.

Interestingly, one can improve on Algorithm 1 by taking the inherent structure of the model into account. Note that in Algorithm 1 the estimator of the generators is not a generator itself. That is, (6) and (7) hold true but in general

$$\int x_j g_j^{t+1}(x_j)\,\mathrm{d}x_j = 0 \text{ and } \int x_j^2 g_j^{t+1}(x_j)\,\mathrm{d}x_j = 1 \tag{9}$$

do *not*. By letting the estimators g^t unconstrained in spite of (6) and (7), information may be lost. To overcome this problem, we propose to base inference on Algorithm 2. Algorithm 2 takes into account the inherent constraints of the model by replacing the standard kernel density estimator (8) by a weighted version (10) satisfying the constraints at each iteration of the algorithm. The proof of pointwise consistency of the the weighted kernel density estimator are postponed to Section 4.

Algorithm 2 proceeds as follows. First one follows the instructions of Algorithm 1 till the construction of the pseudo-samples $\tilde{x}_j^{(i)}$. Then one solves an optimization problem for each marginal to get the weights of an adaptive kernel density estimator which, at each iteration of the algorithm, satisfies the constraints (9) (see Section 4). The optimization problem is convex and easy to solve. Consistency of the resulting estimator is studied in Section 4. Finally, once the marginals have been updated, a last step is added to estimate the copula parameters, as in Algorithm 1.

4 Kernel density estimation under moment constraints

We consider the problem of estimating the common density g of independent random variables $X_1, \ldots, X_n$. We assume that g verifies the regularity conditions in Assumption 1

Assumption 1. *The density g is continuous on $\mathbf{R}$, symmetric about zero and obeys*

$$\int x^2 g(x)\,\mathrm{d}x = 1 \neq \int x^4 g(x)\,\mathrm{d}x < \infty.$$

Note that the assumed symmetry implies

$$\int x g(x) \mathrm{d}x = 0.$$

Algorithm 2

1. Follow the steps 1 and 2 in Algorithm 1.
2. Generate the random labels $Z^{(i)} \sim$ Multi$(w_{i,1}^t, \ldots, w_{i,K}^t)$ and build the pseudo-sample $\tilde{x}_j^i = (x_j^i - \mu_{j,Z^{(i)}}^t)/\sigma_{j,Z^{(i)}}^t$ as in Algorithm 1.
3. Choose a bandwidth h_j and compute

$$\widehat{M}_{n,j} = \begin{pmatrix} 1 & \cdots & 1 \\ x_j^{(1)} & \cdots & x_j^{(n)} \\ [x_j^{(1)}]^2 & \cdots & [x_j^{(n)}]^2 \end{pmatrix}, \text{ and } \mathbf{b}_{n,j} = \begin{pmatrix} 1 \\ 0 \\ 1 - h_j^2 \end{pmatrix}.$$

4. Solve the optimization problems

$$\min_{\mathbf{p} \in \mathbf{R}^n} \|\mathbf{p}\|_2^2$$
$$\text{such that } \begin{cases} \widehat{M}_{n,j}\mathbf{p} = \mathbf{b}_{n,j} \\ \mathbf{p} \geq \mathbf{0}, \end{cases}$$

   and denote the solutions by $\tilde{\mathbf{p}}_j = (\tilde{p}_j^{(1)}, \ldots, \tilde{p}_j^{(n)})$.
5. Follow step 3 of Algorithm 1 but substitute (8) for

$$g_j^{t+1}(x_j) = \frac{1}{h_j} \sum_{i=1}^{n} \tilde{p}_j^{(i)} K\left(\frac{x_j - \tilde{x}_j^{(i)}}{h_j}\right) \tag{10}$$

6. Follow step 4 of Algorithm 1 to update the copula parameters.

Continuity is a standard assumption to ensure pointwise consistency of the standard kernel density estimator [17] and the Nadaraya-Watson estimator [27]. The condition on the moment of second order stems from the structure of the model in Section 2.2. The moment of fourth order must have a different value than that of the moment of second order to ensure the convergence of a certain quantity (see the proof of Theorem 1 for details). We view this rather as a technical condition. For instance if g were the Gaussian density, its variance would have to be not equal to $1/3$.

As explained in Section 3, our aim is to construct an estimator $\hat{g}$ that obeys

$$\int x\hat{g}(x)\,\mathrm{d}x = 0, \text{ and } \int x^2\hat{g}(x)\,\mathrm{d}x = 1. \tag{11}$$

We define the estimator

$$\hat{g}(x) = \sum_{i=1}^{n} \hat{p}_{n,i} K_{h_n}(X_i - x) \tag{12}$$

where $K_{h_n}(y) = K(y/h_n)/h_n$ is a kernel depending on a positive sequence h_n and where $\hat{\mathbf{p}}_n = (\hat{p}_{n,1}, \ldots, \hat{p}_{n,n})'$ (throughout $'$ stands for the transpose operation) is the unique solution of the random optimization problem

$$\min_{\mathbf{p}\in\mathbf{R}_n} \|\mathbf{p}\|_2^2 \tag{13}$$

$$\text{such that } \begin{cases} \widehat{M}_n\mathbf{p} = \mathbf{b}_n \\ \mathbf{p} \geq \mathbf{0}, \end{cases} \tag{14}$$

where $\mathbf{p} = (p_1, \ldots, p_n)'$ and

$$\widehat{M}_n = \begin{pmatrix} 1 & \cdots & 1 \\ X_1 & \cdots & X_n \\ X_1^2 & \cdots & X_n^2 \end{pmatrix}, \text{ and } \mathbf{b}_n = \begin{pmatrix} 1 \\ 0 \\ 1 - h_n^2 \end{pmatrix}.$$

Each $\hat{p}_{n,i}$ is a function of the random sample. For each realization of the sample, the optimization problem (13) is convex and hence admits a unique solution which is denoted by $\hat{\mathbf{p}}_n$. The constraint (14) ensures that $\hat{g}$ satisfies (11). Indeed, elementary calculations show that (11) holds if and only if

$$\sum_{i=1}^{n} \hat{p}_{n,i} X_i = 0 \text{ and } \sum_{i=1}^{n} \hat{p}_{n,i} X_i^2 = 1 - h_n^2,$$

respectively. The constraints $\sum_i \hat{p}_{n,i} = 1$ and $\hat{p}_{n,i} \geq 0$, $i = 1, \ldots, n$, must always hold to ensure that $\hat{g}$ is a density.

As soon as $n > 3$ the system $\widehat{M}_n\mathbf{p} = \mathbf{b}$ has infinitely many solutions and hence there are infinitely many estimators that satisfy (11). We chose to pick the closest one to the standard kernel density estimator. The standard kernel density estimator is an estimator of the form (12) where $\hat{p}_{n,i} = 1/n$, and the solution of

$$\min_{(p_1,\ldots,p_n)} E \int (\sum_{i=1}^{n} p_i K_{h_n}(X_i - x) - g(x))^2\,\mathrm{d}x.$$

In our case, we cannot set $\hat{p}_{n,i} = 1/n$ because the constraint (14) would not be satisfied. But we can project $(1/n, \ldots, 1/n)$ onto the feasible space given in (14), which amounts to solve the optimization problem (13) because minimizing $\|\mathbf{p}\|^2$ is the same as minimizing $\|\mathbf{p} - \mathbf{e}\|^2$, where $\mathbf{e} = (1, \ldots, 1)'$. Thus, the minimization of $\|\mathbf{p}\|_2$ is a heuristic justified by an analogy. Moreover, the minimization of $\|\mathbf{p}\|_2$ is quite convenient from a computational point of view. That said, one can imagine other criteria [6] for choosing $\mathbf{p}$.

Having defined the estimator in (12), it is natural to require at least pointwise consistency. The issue resides in the constraint $\mathbf{p} \geq 0$. Without such a constraint, Lemma 1 states that the solution of the optimization problem is explicit and yields a consistent estimate. In the presence of the constraint, Theorem 1 states that consistency can be achieved under a condition on the tail of the underlying density.

Theorem 1. *Suppose Assumption 1 holds. If $h_n \to 0$, $nh_n \to \infty$ and there exist constants $a_n > 0$, $b_n \in \mathbf{R}$ such that $n^{-1/4}a_n \to 0$, $h_n a_n \to 0$, $n^{-1/4}b_n \to 0$, $h_n b_n \to 0$ and*

$$a_n^{-1}(\max\{X_1, \ldots, X_n\} - b_n) \tag{15}$$

converges in distribution, then the estimator (12) is pointwise consistent.

The conditions $h_n \to 0$ and $nh_n \to \infty$ are necessary to ensure pointwise convergence of the standard kernel density estimator [24]. The condition (15) is standard in extreme value theory [21]. The conditions $n^{-1/4}a_n \to 0$ and $n^{-1/4}b_n \to 0$ state that the rate at which the sample maxima grows to infinity must not be too fast. The conditions $h_n a_n \to 0$ and $h_n b_n \to 0$ state that the rate at which the sample maxima grows to infinity must be smaller than the rate at which the bandwidth h_n vanishes. If h_n is the optimal bandwidth, that is if $h_n \propto n^{-1/5}$, then the conditions $n^{-1/4}a_n \to 0$ and $n^{-1/4}b_n \to 0$ are automatically satisfied. Example 1 and Example 3 give distributions which satisfy these conditions. Example 2 is a counter-example. Example 1 and Example 2 are drawn from [3], p. 153–157. The computation of the normalizing constants in Example 3 is given in the Appendix.

Example 1. *Let $h_n \propto n^{-1/5}$. The Gaussian distribution $(2\pi)^{-1/2}\exp(-x^2/2)$, $x \in \mathbf{R}$, satisfies the conditions in Theorem 1 with*

$$a_n = (2\log n)^{-1/2}, \qquad b_n = \sqrt{2\log n} - \frac{\log(4\pi) + \log\log n}{2(2\log n)^{1/2}}$$

Example 2 (Counter-example)**.** *The Cauchy distribution $g(x) = [\pi(1+x^2)]^{-1}$, $x \in \mathbf{R}$, does* not *satisfy the conditions in Theorem 1. Indeed, in addition to have infinite variance, the normalization constants are given by $a_n = n/\pi$ and $b_n = 0$. The sequence (a_n) does* not *verifies $n^{-1/4}a_n \to 0$.*

Example 3. *Let $h_n \propto n^{-1/5}$. The Laplace distribution $g(x) = \exp(-|x|/b)/(2b)$, $b > 0$, $x \in \mathbf{R}$, satisfies the conditions in Theorem 1 with $a_n = b$ and $b_n = b\log(n/2)$.*

5 Computer experiments

In this section, we wish to compare Algorithm 1 (hereafter called cKDE for convenience) and Algorithm 2 (fKDE) in terms of the quality of the obtained estimates. The standard Gaussian Mixture Model (GMM) was also implemented as a benchmark.

We generated 500 datasets of size 300 according to the following data generating process. The number of clusters was set to $K = 3$ and their proportion parameters were all set of equal value. The Frank family of bivariate copulas, given by

$$C_{\theta_z}(u, v) = -\frac{1}{\theta_z} \log \left(1 + \frac{(e^{-\theta_z u} - 1)(e^{-\theta_z v} - 1)}{(e^{-\theta_z} - 1)} \right), \quad \theta_z \in (-\infty, \infty) \setminus \{0\},$$

was chosen for all of the three copulas. The parameters were $\theta_1 = -3.45$, $\theta_2 = 3.45$ and $\theta_3 = 0$, corresponding to negative, positive and null dependence levels, respectively. The generators for the marginals along the first, resp. second, axis (g_1, resp. g_2), were a normal, resp. a Laplace, distribution with zero mean and unit variance. The three clusters had means ($\mu_{1,1} = -3, \mu_{2,1} = 0$), ($\mu_{1,2} = 0, \mu_{2,2} = 3$) and ($\mu_{1,3} = 3, \mu_{2,3} = 0$) respectively. The scale parameters along the first, resp. second, axis were set to $\sigma_{1,1} = 2$, $\sigma_{1,2} = 0.7$ and $\sigma_{1,3} = 1.4$, resp. $\sigma_{2,1} = 0.7$, $\sigma_{2,2} = 1.4$ and $\sigma_{2,3} = 2.8$. The kernel and the bandwidth selection method used for building the kernel density estimators were the Gaussian kernel and the method given by (3.30) in p. 47 of [24].

In order to compare the algorithms, we computed the mean absolute errors, that is, the differences in absolute value between the true parameters and the estimates. These were averaged over the clusters and the coordinates (if any). For the generators, the L_1 norm was used instead. Only the errors for the location, scale and proportion parameters were computed for GMM. The misclassification rate was computed, too. All these error measures can be computed at each iteration of the algorithms and averaged over the replications. All the three algorithms were run for a fixed number of iterations set arbitrarily to 27 and were initialized according to the nearest neighbour algorithm.

The results are shown in Fig. 1. If one is interested in clustering then the three learning algorithms can be compared on the basis of the misclassification error rate in Fig. 1 (f). The algorithm fKDE did not perform better than GMM even though the last one is misspecified. However, cKDE performed better than both of its competitors. For instance, cKDE yielded a decrease in the median of the misclassification error rates of about 14% (resp. 10%) over GMM (resp. fKDE).

If one is interested in the estimation of the parameters for their own sake, then the error measures considered in Fig. 1 (except the misclassification error rate) are unable to discriminate between GMM and fKDE. Since GMM is misspecified, improvement achieved by fKDE must have occurred elsewhere. For instance, as seen in Fig. 2, the marginal density $f_{2,1}$ has been better estimated with fKDE than with GMM. That said, our interest really resides in the performance of cKDE. And cKDE outperforms both of its competitors and uniformly on all kinds of considered error measures. For instance, cKDE yielded a decrease in the median of the errors for the locations of about 22%, resp. 16%, over GMM, resp. fKDE. The cKDE yielded a decrease in the median of the errors for the scales of about 38%, resp. 18%, over GMM, resp. fKDE. The

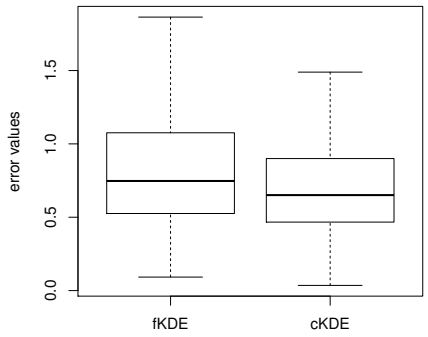

(a) copula parameters

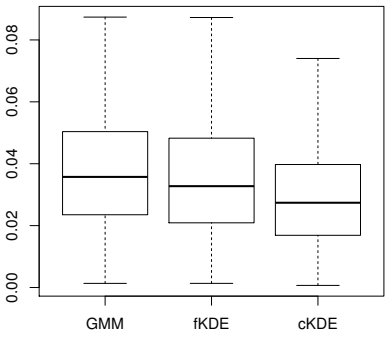

(b) proportion parameters

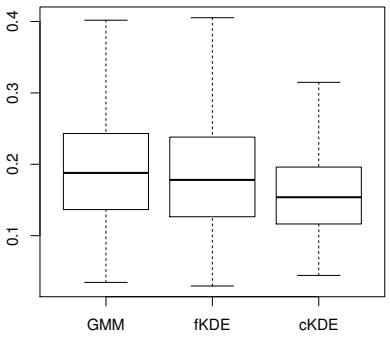

(c) location parameters

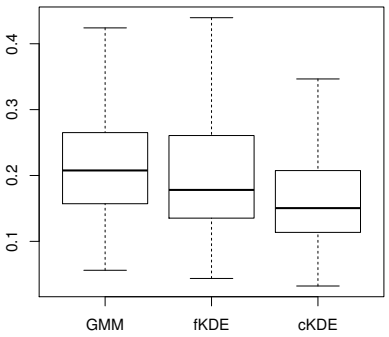

(d) scale parameters

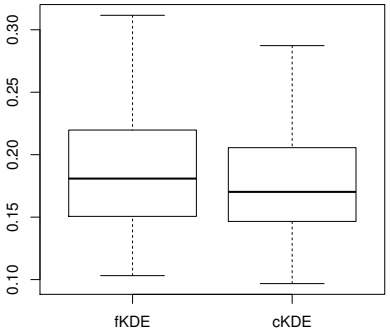

(e) density generators

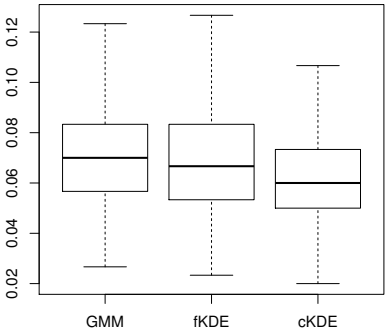

(f) misclassification errors

Figure 1: Boxplots of the error values for the various measures and algorithms.

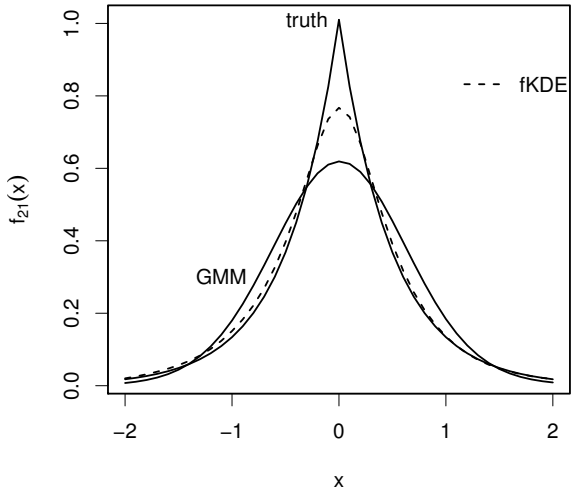

Figure 2: Pointwise averaged marginal density estimates along the second axis in the first cluster for GMM and fKDE. The true underlying density is added for comparison.

algorithm cKDE yielded a decrease in the median of the errors for the copula parameters of about 10% over fKDE. This suggests that building an estimator for the generator that verifies the same constraint as its target, as in Algorithm 2, was a good idea in this context.

Since there is no formal log-likelihood to be relied on, the stability of the algorithms was checked by plotting the pointwise averaged error trajectories. These are displayed in Fig. 3. Note that the lowest trajectory cannot formally be claimed the best because the hypothetical point at which converge the algorithms is unknown. Of course if the sample size is large enough and if the algorithms indeed converge to a consistent estimate then the true parameter would be close to the point at which converge the algorithms. Back to our matter of checking the stability of the algorithms, inspection of Fig. 3 suggests that increasing the number of iterations would not have changed much the insights gained by the computer experiment. The algorithms fKDE and cKDE are very stable for the copula, proportion and location parameters (resp. Fig. 3 (a), Fig. 3 (b) and Fig. 3 (c)). For the scale parameters, the trajectories are stable Fig. 3 (d). For the density generators in Fig. 3 (e), the trajectories are stabilizing.

6 Illustration on RNA-seq data

The use of high-throughput sequencing technologies to sequence ribonucleic acid content results in the production of RNA-seq data. From a statistical point of view, the observations are (realizations of) random variables $Y_{i,j}$, $i = 1, \ldots, n$,

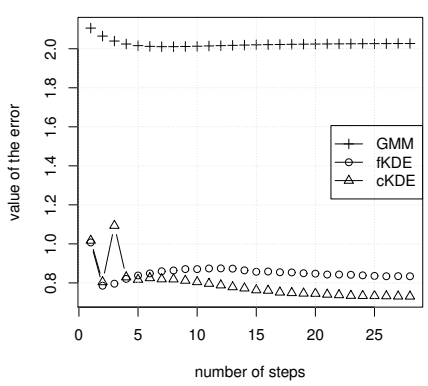

(a) copula parameters

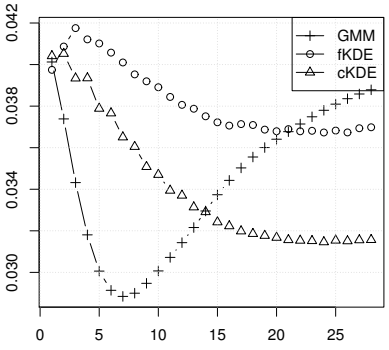

(b) proportion parameters

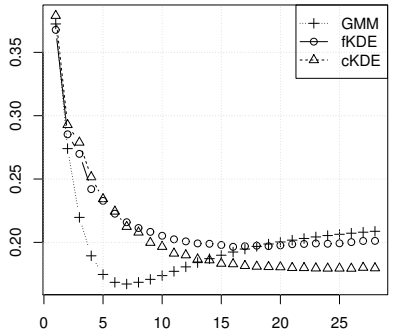

(c) location parameters

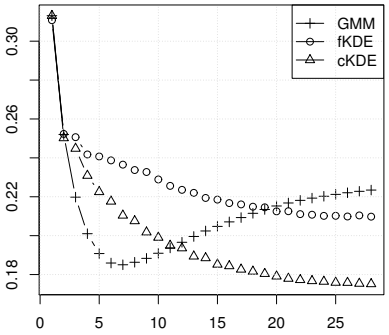

(d) scale parameters

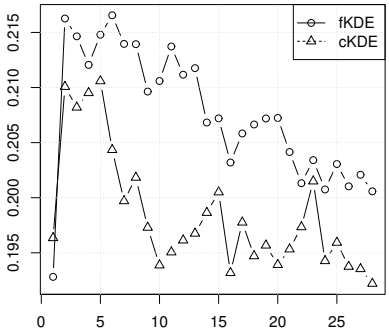

(e) density generators

Figure 3: Trajectories of the pointwise averaged error measures. The x-line is the number of steps and the y-line the value of the error.

$j = 1, \ldots, d$, each of which is a measure of the digital gene expression (DGE) of the biological entity i (e.g., a gene) for the experimental condition j. For instance, $Y_{i,j}$ may be the number of reads of the ith gene for the jth condition aligned to a reference genome sequence. One question of interest deals with the clustering of DGE profiles [19]. For instance, one may want to discover groups of co-expressed genes.

In recent years several clustering methods have been proposed. Poisson mixture models can be applied [19] but they need to assume that, within a cluster, the DGE measures are independent, a very strong assumption. Another approach consists of applying a transformation $Y_{i,j} \mapsto \tilde{Y}_{i,j}$, $i = 1, \ldots, n$, $j = 1, \ldots, d$, so that the transformed data, or pseudo data, are more appropriate for Gaussian mixture models [18]. One such transformation [5] is given by

$$\tilde{Y}_{i,j} = \log\left(\frac{Y_{i,j}/N_j + 1}{m_i + 1}\right),$$

where $N_j = \sum_{i=1}^{n} Y_{i,j}/10^6$ and $m_i = d^{-1}\sum_{j=1}^{d} N_j^{-1} Y_{i,j}$. This approach essentially amounts to assuming that the data are Gaussian on a log-scale. The semiparametric copula-based mixture models permit to relax this assumption.

In this section, we compare the Poisson mixture model of [19], the Gaussian mixture model and the semiparametric copula-based mixture models with Gaussian and Frank copulas. The data are high-throughput transcriptome RNA-seq data [26] downloaded from the companion `R` package `HTSCluster` of [19]. We removed the biological replicates so that $d = 2$. Estimation in the semiparametric copula-based models was performed with Algorithm 2. Estimation in the Poisson mixture model was performed with the function `PoisMixClus` of the package `HTSCluster`. All the algorithms were run with a fixed number of clusters, set to $K = 10$, corresponding to the number of clusters selected by the integrated completed likelihood criterion in the analysis performed in [20].

In order the compare the models, we reproduced Fig. 2 of [19]. The bar heights in Fig. 4 stand for the quantities

$$\frac{\sum_{i=1}^{n} \hat{w}_{i,z} Y_{i,j}}{\sum_{i=1}^{n} \hat{w}_{i,z} \sum_{j=1}^{d} Y_{i,j}},$$

each of which, according to [19], can be interpreted as the proportion of reads that are attributed to condition j in cluster z. The quantities $\hat{w}_{i,z}$ are estimates of the probability that the i-th observation belongs to the z-th cluster, estimate of which depends on the fitted model (Poisson, GMM, or semiparametric copula-based). Bar widths are proportional to $\hat{\pi}_z$, the estimated cluster proportions. Each bar represents a cluster and each color represents a mean normalized expression profile, the value of which is given by the bar length of a given color. In Figure 4, the results for the Poisson model, the only one which does not take into account the dependence structure within the clusters, differ from all the other models. We note that the copula-based semiparametric models are both similar (compared to the Poisson model) and different from GMM. We take this as an encouragement for copula-based semiparametric models: there are not absurd since similar to GMM; there are potentially of practical interest since they differ from GMM.

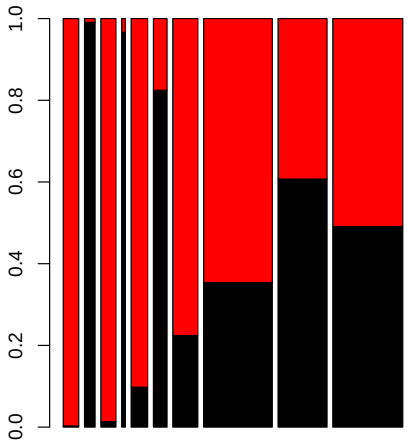

(a) SPC–Frank

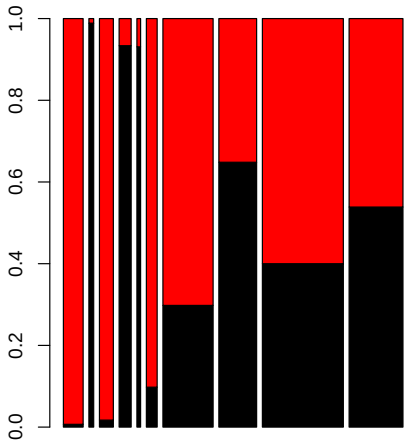

(b) GMM

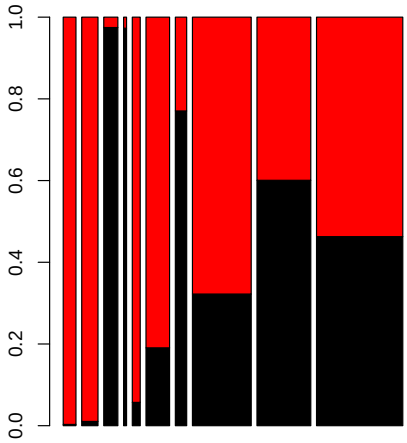

(c) SPC–Gauss

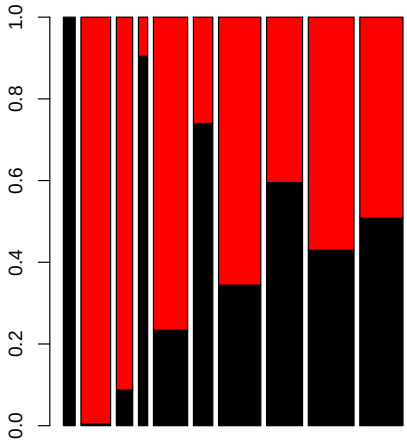

(d) Poisson

Figure 4: Cluster profiles for the Poisson mixture model, the Gaussian mixture model and the semiparametric copula-based mixture models with Frank and Gauss copulas. Each bar represents a cluster and each color represents a mean normalized expression profile, the value of which is given by the bar length of a given color. The bar widths are proportional to the estimated cluster proportions.

7 Summary

We proposed a novel algorithm which permitted to improve the inference in semiparametric copula-based mixture models in which the marginals have a location-scale structure. We did this by replacing the standard kernel density estimator by a weighted one in order to satisfy the inherent constraints of the model. Pointwise consistency of the estimator was proved under mild assumptions. An application on RNA-seq data confirmed the ability of the models to fit real data.

Research on copula-based (and hence genuinely multivariate) semiparametric models has started only recently, and, therefore, many challenges still remain. In particular, the convergence properties of the algorithms in Section 5 or even those in [14, 1, 2] have still to be unraveled, even though a first step has been achieved in [11]. This would open the gate for designing sound convergence check methods and performing model selection (including selection of the correct number of clusters) through pseudo-AIC criteria.

A Appendix

A.1 Computation of the normalizing constants in Example 3

From [3], p. 155, we know that

$$[E(c_n x + d_n; 1/b)]^n \to \Lambda(x), \quad n \to \infty,\, x > 0,$$

where $E(x; 1/b) = 1 - \exp(-x/b)$, $b > 0$ is the distribution function of the exponential distribution, $\Lambda(x) = \exp(-e^{-x})$ is the distribution function of the Gumbel distribution and $c_n = b$, $d_n = b \log n$. Let $L(x; b) = \exp(x/b)/2$, $x > 0$, be the distribution function of the Laplace distribution on the positive real line. Let $a_n = c_n$, $b_n = d_n - b \log 2$ and $x > 0$. By identification of the binomial coefficients in the binomial theorem, we have

$$[L(a_n x + b_n)]^n = [E(c_n x + d_n)]^n \to \Lambda(x),$$

meaning that $a_n = b$ and $b_n = b \log(n/2)$ are the appropriate constants. If $x < 0$, the same formula applies because $a_n x + b_n \to \infty$. □

A.2 Proof of Theorem 1

Theorem 1 shall be proved by first considering the optimization problem (13)–(14) without the constraint $\mathbf{p} \geq \mathbf{0}$. (This shall be called the *simplified* optimization problem.) Throughout the proofs, the bandwidth sequence h_n is simply denoted by h.

Lemma 1. *Let $n \geq 3$. If $h \to 0$ and $nh \to 0$ then the solution $\hat{\mathbf{p}}_n$ of the simplified problem*

$$\min_{\mathbf{p}} \|\mathbf{p}\|_2^2 \tag{16}$$

$$\text{such that } \left\{ \; \widehat{M}_n \mathbf{p} = \mathbf{b}_n \right. \tag{17}$$

obeys

$$\hat{\mathbf{p}}_n = \tilde{\mathbf{p}}_n - \frac{(I - \widetilde{H}_n)\mathbf{X}^2}{\mathbf{X}^{2\prime}(I - \widetilde{H}_n)\mathbf{X}^2}(\mathbf{X}^{2\prime}\tilde{\mathbf{p}}_n - 1 + h^2) \tag{18}$$

$$\tilde{\mathbf{p}}_n = \frac{\overline{X^2}\mathbf{e} - \overline{X}\mathbf{X}}{n(\overline{X^2} - \overline{X}^2)} \tag{19}$$

where $\widetilde{H}_n = \widetilde{M}_n'(\widetilde{M}_n \widetilde{M}_n')^{-1}\widetilde{M}_n$ is the projection matrix on the space spanned by $\mathbf{e}$, $\mathbf{X} = (X_1, \ldots, X_n)$, $\overline{X} = n^{-1}\sum_i^n X_i$, and $\overline{X^2} = n^{-1}\sum_i^n X_i^2$. Moreover, the estimator (12) with $\hat{\mathbf{p}}_n$ as in (16)– (17) is pointwise consistent.

Proof of Lemma 1. Since the distribution of X_i has no atom at zero, one has

$$P(\forall \mathbf{y} \in \mathbf{R}^3,\, \widehat{M}_n'\mathbf{y} \neq \mathbf{0} \text{ or } \mathbf{y} = \mathbf{0}) = 1,$$

meaning that $\widehat{M}_n'$ has full rank with probability one. Since $n \geq 3$ this rank must be three. Hence $\widehat{M}_n\widehat{M}_n'$ has full rank equal to three and therfore is invertible. The optimization problem is convex hence there is a unique solution $\hat{\mathbf{p}}_n$ whose expression is easily found: the Lagrangian writes $\mathbf{p}'\mathbf{p} - \lambda(\widehat{M}_n - \mathbf{b}_n)$ for some $\lambda > 0$ and by equating its gradient to zero we get

$$\hat{\mathbf{p}}_n = \widehat{M}_n'(\widehat{M}_n\widehat{M}_n')^{-1}\mathbf{b}_n \tag{20}$$

(and $\lambda = 2(\widehat{M}_n\widehat{M}_n')^{-1}\mathbf{b}_n$).

In order to obtain the desired formulas (18) and (19) it is convenient to introduce

$$\widetilde{M}_n = \begin{pmatrix} 1 & \cdots & 1 \\ X_1 & \cdots & X_n \end{pmatrix} \text{ and } \mathbf{X}^2 = \begin{pmatrix} X_1^2 \\ \vdots \\ X_n^2 \end{pmatrix}.$$

so that we have the decompositions by blocks:

$$\widehat{M}_n = \begin{pmatrix} \widetilde{M}_n \\ \mathbf{X}^{2\prime} \end{pmatrix} \text{ and } \widehat{M}_n\widehat{M}_n' = \begin{pmatrix} \widetilde{M}_n\widetilde{M}_n' & \widetilde{M}_n\mathbf{X}^2 \\ \mathbf{X}^{2\prime}\widetilde{M}_n' & \mathbf{X}^{2\prime}\mathbf{X}^2 \end{pmatrix}.$$

Let $\widetilde{H}_n = \widetilde{M}_n'(\widetilde{M}_n\widetilde{M}_n')^{-1}\widetilde{M}_n$ be the projection matrix onto the linear space spanned by the rows of $\widetilde{M}_n$. With this notation, we have

$$[\widehat{M}_n\widehat{M}_n']^{-1} = \begin{pmatrix} (\widetilde{M}_n\widetilde{M}_n')^{-1} + \frac{(\widetilde{M}_n\widetilde{M}_n')^{-1}\widetilde{M}_n\mathbf{X}^2\mathbf{X}^{2\prime}\widetilde{M}_n'(\widetilde{M}_n\widetilde{M}_n')^{-1}}{\mathbf{X}^{2\prime}(I-\widetilde{H}_n)\mathbf{X}^2} & \frac{-(\widetilde{M}_n\widetilde{M}_n')^{-1}\widetilde{M}_n\mathbf{X}^2}{\mathbf{X}^{2\prime}(I-\widetilde{H}_n)\mathbf{X}^2} \\ \frac{-\mathbf{X}^{2\prime}\widetilde{M}_n'(\widetilde{M}_n\widetilde{M}_n')^{-1}}{\mathbf{X}^{2\prime}(I-\widetilde{H}_n)\mathbf{X}^2} & \frac{1}{\mathbf{X}^{2\prime}(I-\widetilde{H}_n)\mathbf{X}^2} \end{pmatrix}$$

Decomposing $\mathbf{b}_n = (\tilde{\mathbf{b}}_n', 1-h^2)'$ and applying formula (20) then yields (18) with $\tilde{\mathbf{p}}_n = \widetilde{M}_n'(\widetilde{M}_n\widetilde{M}_n')^{-1}\tilde{\mathbf{b}}_n$, this last equality being equivalent to (19).

We now introduce an intermediate lemma in order to facilitate the study of remainder terms which shall appear in the proof of consistency.

Lemma 2. *Let $(Z_{n,1}, \ldots, Z_{n,n})$ be i.i.d. random variables defined on the same probability space as $X_1, \ldots, X_n$. They are assumed to obey $n^{-1}\sum_{i=1}^n Z_{n,i}X_i^k \to c_k$, $k = 0, 1, 2$, in probability as $n \to \infty$ where c_k is some real constant. Then*

$$\frac{1}{n}\mathbf{X}^{2\prime}(I - \widetilde{H}_n)\mathbf{Z}_n \xrightarrow{P} c_2 - c_0, \quad n \to \infty,$$

where $\mathbf{Z}_n = (Z_{n,1}, \ldots, Z_{n,n})'$.

Proof of Lemma 2. Write

$$\frac{1}{n}\mathbf{X}^{2\prime}(I - \widetilde{H}_n)\mathbf{Z}_n = \frac{1}{n}\sum_{i=1}^n X_i^2 Z_{n,i} - \frac{1}{n}\mathbf{X}^{2\prime}\widetilde{M}_n' n(\widetilde{M}_n\widetilde{M}_n')^{-1}\frac{1}{n}\widetilde{M}_n\mathbf{Z}_n \xrightarrow{P} c_2 - c_0.$$

To see why the limit holds, note that $n(\widetilde{M}_n\widetilde{M}_n')^{-1}$ converges elementwise to the identity matrix.

We now prove the consistency statement of Lemma 1. We have $\hat{g}(x) = \tilde{g}(x) + \hat{g}(x) - \tilde{g}(x)$ with $\tilde{g}(x) = \sum_{i=1}^n \tilde{p}_{n,i}K_h(x - X_i)$ and $\hat{g}(x) - \tilde{g}(x) = \sum_{i=1}^n(\hat{p}_{n,i} -$

$\tilde{p}_{n,i})K_h(x-X_i)$. Using (19) and $\sum_{i=1}^n X_i K_h(x-X_i)/\sum_{i=1}^n K_h(x-X_i) \to x$, we easily get that $\tilde{g}(x) \to g(x)$ in probability. Now using (19)–(20) and Lemma 2 we also get

$$\hat{g}(x) - \tilde{g}(x) = \frac{\mathbf{X}^{2\prime}\tilde{\mathbf{p}}_n + 1 - h^2}{\mathbf{X}^{2\prime}(I - \widetilde{H}_n)X^2}\mathbf{X}^{2\prime}(I - \widetilde{H}_n)K \xrightarrow{P} 0,$$

where $K = (K_h(x-X_1), \ldots, K_h(x-X_n))'$. The proof of Lemma 1 is complete. □

Proof of Theorem 1. In this proof, the symbol $\hat{\mathbf{p}}_n$ stands for the solution of the optimization problem (16)–(17), that is, *without* the positivity constraint, and the symbol $\hat{\mathbf{p}}_n^+$ stands for the solution of the optimization problem (13)–(14), that is, *with* the positivity constraint. In view of Lemma 1, it is sufficient to show that

$$P(\hat{p}_{n,i} \geq 0,\, i = 1, \ldots, n) \to 1, \quad n \to \infty,$$

because, by definition of the optimization problems, this implies that

$$P(\hat{p}_{n,i} = \hat{p}_{n,i}^+,\, i = 1, \ldots, n) \to 1$$

and therefore that the estimators are equal with probability tending to one.

We write

$$\hat{p}_{n,i} = \tilde{p}_{n,i}\left(1 + \frac{\hat{p}_{n,i} - \tilde{p}_{n,i}}{\tilde{p}_{n,i}}\right)$$

and the proof will be complete if (i) $P(\tilde{p}_{n,i} \geq 0,\, i = 1, \ldots, n) \to 1$ and (ii) $|(\hat{p}_{n,i} - \tilde{p}_{n,i})/\tilde{p}_{n,i}|$ can be bounded above by a quantity which would not depend on i and would vanish asymptotically.

We first show (i). We have

$$|n\tilde{p}_{n,i} - 1| = \left|\frac{\overline{X}^2 - \overline{X}X_i}{\overline{X^2} - \overline{X}^2}\right| \leq \left|\frac{\overline{X}^2}{\overline{X^2} - \overline{X}^2}\right| + \left|\frac{\overline{X}}{\overline{X^2} - \overline{X}^2}a_n a_n^{-1}X_i\right|.$$

The first term in the right hand side is a $O_P(n^{-1})$ and does not depend on i. Now

$$\begin{aligned}
|a_n^{-1}X_i| \leq & \vee_i |a_n^{-1}X_i| \\
= & \max\{\vee_i a_n^{-1}X_i, \vee_i - a_n^{-1}X_i\} \\
= & \max\{\vee_i a_n^{-1}(X_i - b_n), \vee_i - a_n^{-1}(X_i + b_n)\} + a_n^{-1}b_n,
\end{aligned}$$

where $\vee_i X_i$ is a compact notation for $\max\{X_1, \ldots, X_n\}$. By assumption, $\vee_i a_n^{-1}(X_i - b_n)$ converges in distribution. By symmetry, so does $\vee_i - a_n^{-1}(X_i + b_n)$. Hence, by the continuous mapping theorem, the maximum of $\vee_i a_n^{-1}(X_i - b_n)$ and $\vee_i - a_n^{-1}(X_i + b_n)$ converges in distribution. Thus

$$\begin{aligned}
|n\tilde{p}_{n,i} - 1| \leq & \left|\frac{\overline{X}^2}{\overline{X^2} - \overline{X}^2}\right| + \\
& \left|\frac{\overline{X}}{\overline{X^2} - \overline{X}^2}a_n\right| |\max\{\vee_i a_n^{-1}(X_i - b_n), \vee_i - a_n^{-1}(X_i + b_n)\} + a_n^{-1}b_n| \\
= & O_P(n^{-1}) + O_P(n^{-1/2}a_n)(O_P(1) + a_n^{-1}b_n).
\end{aligned}$$

The bound does not depend on i and vanishes asymptotically in probability by assumption on the sequences a_n and b_n. This is enough to conclude that (i) holds with probability tending to one.

We finally show (ii). It is convenient to introduce Lemma 3 the proof of which is deferred to the end of this Section.

Lemma 3. *Let v_n be a positive sequence satisfying $v_n^{-1} \to 0$, $v_n^{-1}a_n \to 0$, $v_n^{-1}b_n \to 0$. There exist random quantities A_n, B_n, C_n, D_n, E_n such that, as $n \to \infty$, A_n is $O_P(v_n^{-2})$, B_n, C_n, D_n are $O_P(v_n^{-1})$, E_n tends to a nonzero constant in probability, $P(D_nX_i + E_n > 0,\, i = 1, \ldots, n) \to 1$ and*

$$\frac{\hat{p}_{n,i} - \tilde{p}_{n,i}}{\tilde{p}_{n,i}} = \frac{A_nX_i^2 + B_nX_i + C_n}{D_nX_i + E_n} \tag{21}$$

In view of 21, one has

$$\left|\frac{\hat{p}_{n,i} - \tilde{p}_{n,i}}{\tilde{p}_{n,i}}\right| \leq \frac{|A_n| \vee_{i=1}^n X_i^2 + |B_n| \vee_{i=1}^n X_i + |C_n|}{E_n - \vee_{i=1}^n - D_nX_i} \tag{22}$$

(we used the fact that $\min\{y_1, \ldots, y_n\} = -\max\{-y_1, \ldots, -y_n\}$ for the denominator). By assumption and by symmetry, both $\vee_{i=1}^n X_i$ and $\vee_{i=1}^n - X_i$ are $O_P(a_n) + b_n$ and by assumption on v_n,

$$v_n^{-2} \vee_{i=1}^n X_i^2 = \left[\max(v_n^{-1} \vee_{i=1}^n X_i, v_n^{-1} \vee_{i=1}^n -X_i)\right]^2 \xrightarrow{P} 0.$$

Hence the numerator in (22) is $o_P(1)$. The denominator equals $E_n + D_n \vee_{i=1}^n X_i$ if $D_n < 0$ and equals $E_n - D_n \vee_{i=1}^n -X_i$ if $D_n > 0$. Either way, the denominator tends to a constant in probability and

$$\left|\frac{\hat{p}_{n,i} - \tilde{p}_{n,i}}{\tilde{p}_{n,i}}\right| \leq$$

$$\max\left\{\frac{|A_n| \vee_{i=1}^n X_i^2 + |B_n| \vee_{i=1}^n X_i + |C_n|}{E_n + D_n \vee_{i=1}^n X_i}, \frac{|A_n| \vee_{i=1}^n X_i^2 + |B_n| \vee_{i=1}^n X_i + |C_n|}{E_n - D_n \vee_{i=1}^n -X_i}\right\}.$$

This upper bound does not depend on i and vanishes asymptotically in probability. This proves (ii). It only remains to prove Lemma 3.

Proof of Lemma 3. Let $\delta_{i,j} = 1$ whenever $i = j$ and $\delta_{i,j} = 0$ whenever $i \neq j$. Let $\widetilde{H}_{i,j}$ denote the element at the i-th row and j-th column of $\widetilde{H}_n$. We have

$$\frac{\hat{p}_{n,i} - \tilde{p}_{n,i}}{\tilde{p}_{n,i}} = \frac{-\sum_{j=1}^n (\delta_{i,j} - \widetilde{H}_{i,j}) X_j^2 \frac{\mathbf{X}^{2\prime}\tilde{\mathbf{p}}_n - 1 + h^2}{\mathbf{X}^{2\prime}(I - \widetilde{H}_n)\mathbf{X}^2}}{\frac{\overline{X^2} - \overline{X}\,\overline{X_i}}{n(\overline{X^2} - \overline{X}^2)}}.$$

Standard calculations yield

$$\sum_{j=1}^n (\delta_{i,j} - \widetilde{H}_{i,j}) X_j^2 = \frac{(\overline{X^2} - \overline{X}^2)X_i^2 + (\overline{X}\,\overline{X^2} - \overline{X^3})X_i + \overline{X}\,\overline{X^3} - \overline{X^2}^2}{\overline{X^2} - \overline{X}^2}$$

and hence we can rewrite

$$\frac{\hat{p}_{n,i} - \tilde{p}_{n,i}}{\tilde{p}_{n,i}} = \frac{[-(\overline{X^2} - \overline{X}^2)X_i^2 - (\overline{X}\,\overline{X^2} - \overline{X^3})X_i - \overline{X}\,\overline{X^3} + \overline{X^2}^2][\mathbf{X}^{2\prime}\tilde{\mathbf{p}}_n - 1 + h^2]}{[\overline{X^2} - \overline{X}X_i][n^{-1}\mathbf{X}^{2\prime}(I - \widetilde{H}_n)\mathbf{X}^2]}.$$

This is a ratio of polynomials in X_i that can be identified with (21). One easily sees that $\mathbf{X}^{2\prime}\tilde{\mathbf{p}}_n - 1 + h^2$ is $O_P(n^{-1/2}) + O_P(h^2)$ and hence all the coefficients of the polynomial in the numerator are (at least) $O_P(n^{-1/2}) + O_P(h^2)$. By Lemma 2, $n^{-1}\mathbf{X}^{2\prime}(I - \widetilde{H}_n)\mathbf{X}^2$ tends to $EX_1^4 - 1$ which nonzero by assumption. Therefore the desired equation (21) is satisfied with

$$
\begin{aligned}
v_n^{-2} &= n^{-1/2} + h^2, \\
A_n &= -(\overline{X^2} - \overline{X}^2)[\mathbf{X}^{2\prime}\tilde{\mathbf{p}}_n - 1 + h^2] \\
B_n &= -(\overline{X}\,\overline{X^2} - \overline{X^3})[\mathbf{X}^{2\prime}\tilde{\mathbf{p}}_n - 1 + h^2] \\
C_n &= (-\overline{X}\,\overline{X^3} + \overline{X^2}^2)[\mathbf{X}^{2\prime}\tilde{\mathbf{p}}_n - 1 + h^2] \\
E_n &= \overline{X^2} n^{-1}\mathbf{X}^{2\prime}(I - \widetilde{H}_n)\mathbf{X}^2.
\end{aligned}
$$

Indeed, $v_n^{-2}a_n^2 = n^{-1/2}a_n^2 + h^2 a_n^2 \to 0$ by the assumptions in Theorem 1. Let us show that A_n is $O_P(v_n^{-2})$. We have

$$
\begin{aligned}
v_n^2 A_n =& O_p(v_n^2 n^{-1/2}) + O_p(v_n^2 h^2) \\
=& O_p\left(\frac{1}{1 + n^{1/2}h^2}\right) + O_p\left(\frac{1}{1 + n^{-1/2}h^{-2}}\right) \\
=& O_p(1),
\end{aligned}
$$

the last equality holding because the sequence $(1 + n^{1/2}h^2)^{-1}$ is bounded. The remaining conditions in Lemma 3 are checked in the same way. The proof of Lemma 3 is complete. Hence the proof of Theorem 1 is complete, too. □

References

[1] T. Benaglia, D. Chauveau, and D. R. Hunter. An EM-like algorithm for semi- and nonparametric estimation in multivariate mixtures. *Journal of Computational and Graphical Statistics*, 18(2):505–526, 2009.

[2] L. Bordes, D. Chauveau, and P. Vandekerkhove. A stochastic EM algorithm for a semiparametric mixture model. *Computational Statistics & Data Analysis*, 51, 2007.

[3] P. Embrechts, C. Klüppelberg, and T. Mikosch. *Modelling Extremal Events for Insurance and Finance*. Springer, 1997.

[4] R. Fujimaki, Y. Sogawa, and S. Morinaga. Online heterogeneous mixture modeling with marginal and copula selection. In *Proceedings of the 17th ACM SIGKDD International Conference on Knowledge Discovery and Data Mining*, KDD '11, pages 645–653, New York, NY, USA, 2011. ACM.

[5] M. Gallopin. *Classification et inférence de réseaux pour les donneées RNA-seq*. PhD thesis, Université Paris-Saclay, 2015.

[6] P. Hall and B. A. Turlach. Reducing bias in curve estimation by use of weights. *Computational Statistics & Data Analysis*, 30(1):67 – 86, 1999.

[7] H. Hu, Y. Wu, and W. Yao. Maximum likelihood estimation of the mixture of log-concave densities. *Computational Statistics & Data Analysis*, 101:137–147, 2016.

[8] D. Kim, J.-M. Kim, S.-M. Liao, and Y.-S. Jung. Mixture of D-vine copulas for modeling dependence. *Computational Statistics & Data Analysis*, 64:1–19, 2013.

[9] I. Kosmidis and D. Karlis. Model-based clustering using copulas with applications. *Statistics and Computing*, pages 1–21, 2015.

[10] S. Lee and G. J. McLachlan. Finite mixtures of multivariate skew t-distributions: some recent and new results. *Statistics and Computing*, 24(2):181–202, 2014.

[11] M. Levine, D. R. Hunter, and D. Chauveau. Maximum smoothed likelihood for multivariate mixtures. *Biometrika*, 98(2):403–416, 2011.

[12] P. K. Mallapragada, R. Jin, and A. Jain. Nonparametric mixture models for clustering. In *Joint IAPR International Workshop, SSPR & SPR 2010*, volume 6218, pages 334–343. Springer, Hancock, E. R. and Wilson, R. C. and Windeatt, T. and Ulusoy, I. and Escolano, F., 2010.

[13] M. Marbac, C. Biernacki, and V. Vandewalle. Model-based clustering of Gaussian copulas for mixed data. *Communications in Statistics - Theory and Methods*, 46(23):11635–11656, 2017.

[14] G. Mazo. A semiparametric and location-shift copula-based mixture model. *Journal of Classification*, 34(3):444–464, 2017.

[15] G. McLachlan and D. Peel. *Finite mixture models*. John Wiley & Sons, 2004.

[16] R. B. Nelsen. *An introduction to copulas*. Springer, 2006.

[17] E. Parzen. On estimation of a probability density function and mode. *Ann. Math. Statist.*, 33:1065–1076, 1962.

[18] A. Rau and C. Maugis-Rabusseau. Transformation and model choice for rna-seq co-expression analysis. *Briefings in Bioinformatics*, page bbw128, 2017.

[19] A. Rau, C. Maugis-Rabusseau, M.-L. Martin-Magniette, and G. Celeux. Co-expression analysis of high-throughput transcriptome sequencing data with poisson mixture models. *Bioinformatics*, 31(9):1420–1427, 2015.

[20] A. Rau, C. Maugy-Rabusseau, M.-L. Martin-Magniette, and G. Celeux. *Co-expression analysis of RNA-seq data with the HTSCluster package*. Version 2.0.8. User guide for the HTSCluster accessible from within R.

[21] S. I. Resnick. *Extreme values, regular variation and point processes*. Springer, 2013.

[22] M. Rey and V. Roth. Copula mixture model for dependency-seeking clustering. In *Proceedings of the 29-th International Conference on Machine Learning*, 2012.

[23] A. Roy and S. K. Parui. Pair-copula based mixture models and their application in clustering. *Pattern Recognition*, 47(4):1689 – 1697, 2014.

[24] B. W. Silverman. *Density estimation for statistics and data analysis*. Chapman & Hall, 1998.

[25] A. Sklar. Fonction de répartition dont les marges sont données. *Inst. Stat. Univ. Paris*, 8:229–231, 1959.

[26] M. Sultan, M. H. Schulz, H. Richard, A. Magen, A. Klingenhoff, M. Scherf, M. Seifert, T. Borodina, A. Soldatov, D. Parkhomchuk, D. Schmidt, S. O'Keeffe, S. Haas, M. Vingron, H. Lehrach, and M.-L. Yaspo. A global view of gene activity and alternative splicing by deep sequencing of the human transcriptome. *Science*, 321(5891):956–960, 2008.

[27] G. S. Watson. Smooth regression analysis. *Sankhyā Ser. A*, 26:359–372, 1964.